"Studies on the Preparation and Application of Multifunctional Nano Structured Materials"

Synopsis of Work (5000 Words)

For the Award of Ph. D. (Sc.) Degree in Chemistry

Submitted to

The Presidency University

By

Arindam Das

Registration Number: R-19RS205120254

Date of Registration: 25/6/2021

Presidency University

Co-Supervisor

Dr. Dhruba Prosad Chatterjee

Associate Professor

Department of Chemistry

Presidency University

Mr. Arindam Das has successfully defended his WORK therefore, we recommend submission of his Ph.D. thesis.

Chhanda Mukhopadhyay 18/9/24

Sujoy Baitalik 18/09/2024

Supervisor

Dr. Biplab Biswas

Assistant Professor

Department of Chemistry

Presidency University

D Bhattacharjee 18/09/2024

Aditya Bose

18/9

Contents	Page No.
Chapter 1 (Introduction)	**3-9**
Chapter 2 (Pivotal Role of Oligoanilines as Regulator of Polyaniline Chain Growth, Helicity and Overall Morphology)	**10-14**
Chapter 3 (Polyaniline-(dinonylnapthyl disulphonic acid) hydrogel showing enhanced supercapacitor and photo-current performance by in situ growth of AgNPs)	**15-26**
Chapter 4 (Preparation of Highly Efficient 3D Network Structured Pyrolyzed Graphene Oxide/Polyaniline Composite Electrode for Flexible Supercapacitor)	**27-30**
Chapter 5 (Summary of research work and future objectives)	**31-33**
References	**34-36**
List of publications and papers presented in conferences	**36-37**

Chapter 1

Introduction

Nanostructured materials have garnered significant interest for their applications across diverse fields. Their remarkable properties specifically high surface area, enhanced mechanical strength, improved optical and electrical properties have made them highly attractive for a wide range of applications across different industries.[1,2,3]

Supercapacitors, also known as ultracapacitors or electrochemical capacitors are a notable class of components in the landscape of energy storage technologies. Distinguished by their rapid charge-discharge process (typically in minutes), supercapacitors can endure millions of charge-discharge cycles due to high power density.[3,4] Supercapacitors have longer cycle life compared to batteries, making them steadfast for construction of long-term energy storage device. (Scheme 1.1) In the context of energy storage performance nanostructured material has been found to be well-suited for supercapacitor applications. These materials offer high surface area, high electrical conductivity, short diffusion pathways for ions, which are crucial for improving supercapacitor performances.[3,4]

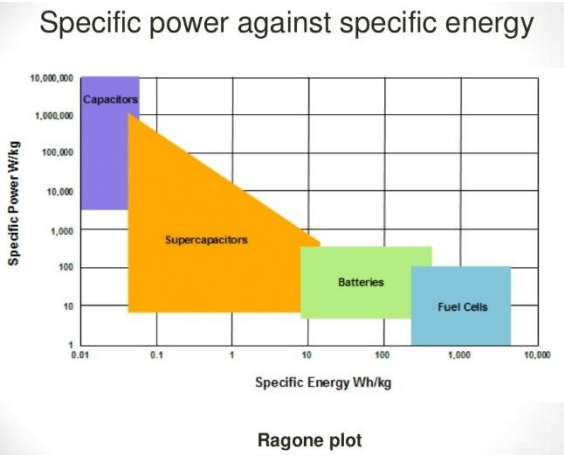

Scheme1.1. Simplified Ragone plot of the energy storage domains for the various electrochemical energy conversion systems compared to an internal combustion engine and turbines and conventional capacitors.

Conducting polymers (CPs) have revolutionized the field of supercapacitors owing to their inherent electrical conductivity and pseudocapacitance. CPs can store energy while keeping the flexibility and processability of traditional polymers, which is in sharp contrast to other conventional conductive materials like carbon nanomaterials.[4] CPs primarily store charge by pseudocapacitive redox process involving reversible insertion and extraction of ions throughout the polymer matrix.[4] It sets them apart from EDLC where charge is stored in the interface of electrode and electrolyte. Pseudocapacitive results in high specific capacitance value owing to the faradaic reactions within the polymer whereas the EDLC results from electrostatic non-faradaic charge accumulation in the electrode-electrolyte interface, making their specific capacitance lower than pseudocapacitive materials.[4] Polyaniline (PANI), a conducting polymer known for its high theoretical capacitance, easy synthesis has been widely investigated as a pseudocapacitive material for supercapacitor applications.[4,5] PANI offers a high specific capacitance resulting from fast redox reactions at the electrode-electrolyte interface, thereby enhancing the overall energy storage capacity of the supercapacitor. Polyaniline is typically synthesized in an aqueous acidic medium, in presence of oxidant Ammonium peroxo disulphate (APS).[6]

PANI hydrogel have garnered significant attention for supercapacitor application owing to their high porosity, large surface area, long cyclic stability.[7] The high water-content in hydrogels results in tremendous flexibility, which makes them a promising material for the fabrication of flexible supercapacitor device. Furthermore, the porous PANI hydrogels facilitates faster ion diffusion and the interconnected network in polymer matrix allow efficient electrolyte penetration and ion transport, enabling rapid charge/discharge process and high power density.[8]

PANI hydrogels can be prepared by various methods by using phytic acid, folic acid or by using surfactants such as dinonyl napthyl sulphonic acid, dinonylnapthyl disulphonic acid, camphor sulphonic acid.[9-13] A report by Das *et.al* indicates that incorporation of silver

nanoparticles within PANI hydrogel framework increases electrochemical performance of the hydrogel.[10,] It is due to the high surface area and conductivity of the AgNPs that the electrode performance is enhanced.[10] Also, the rigid AgNPs withstand the volume degradation during rapid charge discharge process, which results in the increase of cyclic stability of the hydrogels.[10]

In one of the study of the present thesis, dinonylnapthyl disulphonic acid (DNNDSA) doped PANI hydrogel has been synthesized for supercapacitor application and demonstration of photoresponse properties. Introduction of AgNPs in fibrillar hydrogel network increases the electrode performance as well as photocurrent photoswitching properties, which is attributed to the synergistic interaction between polaronic band of PANI and plasmon band of AgNPs. In this novel approach DNNDSA-PANI hydrogel composites were synthesized for the first time in in aqueous medium by simple oxidative polymerization of aniline by APS.

The autocatalytic oxidative polymerization of aniline exhibits that the oxidation potential for conversion of monomeric aniline to dimeric *N*-phenyl- 1,4 phenylenediamine (*p*-semidine) is 0.9V, which sharply decreases to (0.4-0.6) V during the subsequent formation of trimeric N,N'-bis(4'-aminophenyl)-1,4-quinonediimine (APQD).[6,14,15]**(Scheme 1.2)**

Oxidation potential decreases consistently with the formation of higher aniline oligomers. One of the main challenges in using PANI is its mechanical degradation over time, which can be attributed to the swelling and shrinking during charge-discharge cycles.[16] To solve this problem research has been focused on improving the mechanical integrity of the PANI chains through developing novel composites with carbon materials.[17] In this process the rigid carbon materials can accommodate the volume changes during multiple charge-discharge cycles without losing electrical conductivity.[6,16,17]

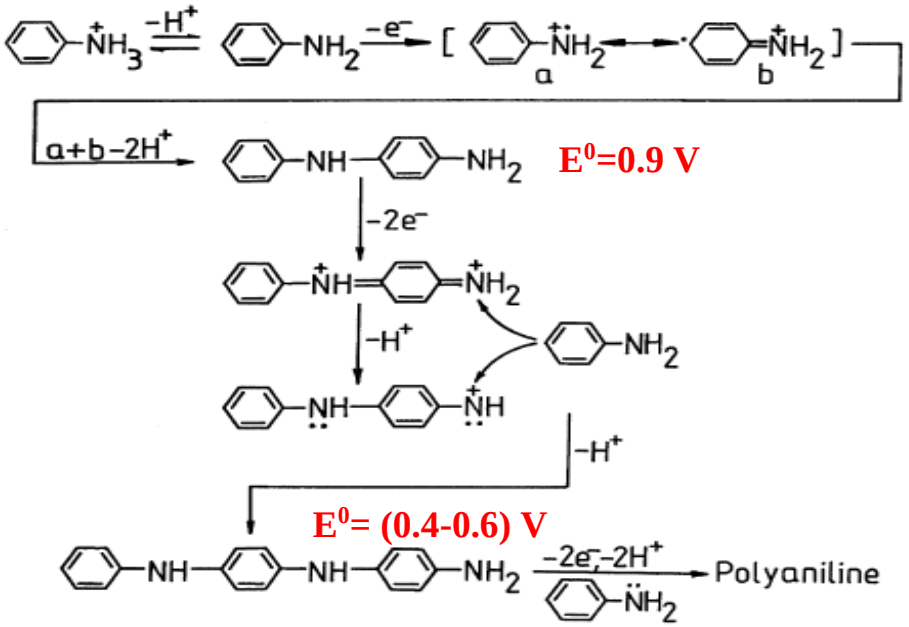

Scheme 1.2. Oxidative polymerization of aniline[6,14]

Carbon-based nanomaterials have garnered significant attention as promising electrode materials for supercapacitors due to their high surface area, excellent electrical conductivity, mechanical strength, and long cycle life.[4] 2D graphene sheets, hold great potential as EDLC materials due to their exceptionally high theoretical surface area, specific capacitance, conductivity, and mechanical strength.[4] Nonetheless, the main challenges associated with their widespread application is their high production cost and complex preparative methods. Though, graphene oxide (GO) sheets can be produced cost-effectively on a large scale; however, their low conductivity restricts charge storage properties. Although reduction of GO sheets through chemical methods restores conductivity but restacking of sheets and presence of oxygen-containing fuctionalities including epoxy, carboxy, hydroxyl groups negatively impact conductivity.[4,18] Thermally reducing GO sheets at high temperatures is a more effective approach, as it efficiently eliminates oxygen functionalities and creates void spaces through which the charge can be percolate.[18] Carbon nanotubes (CNTs) represent another type of 1D carbonaceous nanomaterial which have garnered significant interest as EDLC electrodes owing

to their exceptionally high experimental conductivity and theoretical surface area. **(Scheme 1.3)** Several studies have reported the enhanced electrochemical properties of graphene or reduced graphene oxide (r-GO)/carbon nanotube (CNT) nanocomposite materials when used as supercapacitor electrodes. Dai et al. developed 3D nanostructured materials by integrating 2D pyrolyzed graphene sheets with 1D CNTs, where the CNTs are vertically organized between the 2D graphene sheets.[19] In another study, Zhang et al. demonstrated that reduced GO/CNT composites incorporating super short CNTs (SSCNTs) with an aspect ratio of less than 5 exhibit significantly better capacitive performance compared to multi-walled CNTs (MWCNTs).[20] Zero dimensional graphene oxide quantum dot (GQD) supramolecularly attached with PANI nano rods[21] have reportedly produced very high specific capacitance. Similarly, carbonized GQD used as electrode performed efficiently.[22] In numerous literature reports, covalent linkage of PANI chains to carbon nanomaterials has been achieved through the initiation of PANI chain growth from aniline moieties tethered to the surfaces of the carbon nanomaterials.[5,16,17] Nevertheless, under those conditions, there remains a concern regarding the potential for uncontrolled PANI chain growth resulting from competitive homogenous nucleation within the polymerization bulk. In this regard, if polymerization is initiated from oligomer nucleates, then more control would be exerted in the polymerization reaction. It is

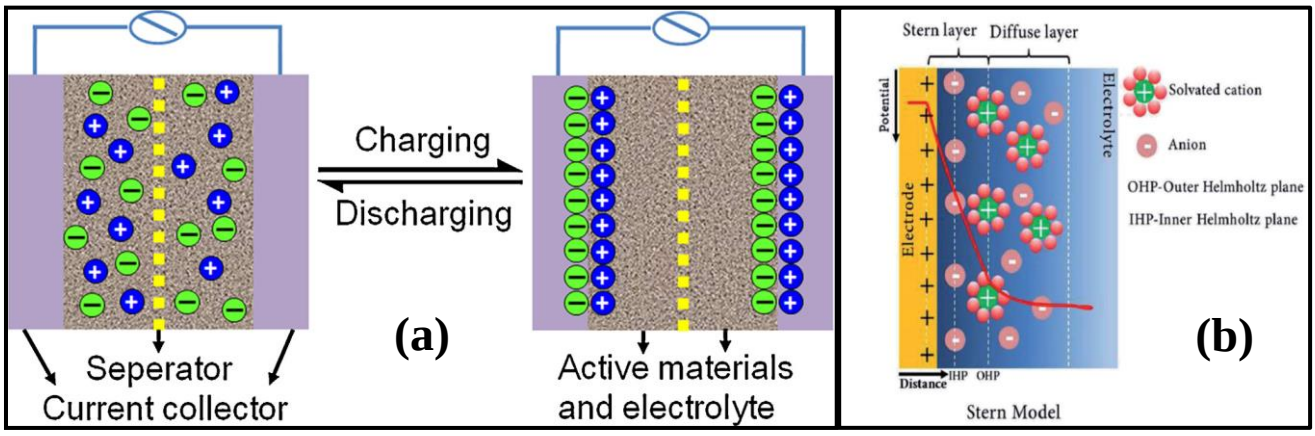

Scheme 1.3 (a) Schematic illustration of the charging/discharging process in a supercapacitor; (b) Representation of EDLC structure: Gouy–Chapman–Stern model.[26]

worth noting within this framework that a previous study has reported an acceleration of rate of polymerization of aniline in presence of aniline oligomer.[23] In this regard, previous reports have highlighted that APQD has been anchored to carbon materials through covalent bonding.[24,25] The PANI-composite materials linked through covalent bonds demonstrated enhanced electrochemical properties and marked increase in reaction rate in comparison to the composites that were not covalently attached by APQD. But these composites have been synthesized through lengthy and complicated chemical routes with multiple steps. Hence, an easy synthetic method accompanied with time-efficient chemical pathway is imperative.

In our current study, our primary aim was to fabricate a 3D graphene/polyaniline (PANI) nanocomposite through combination of highly conducting pyrolyzed 2D graphene sheets with 1D PANI nanotubes. This was achieved through the in-situ synthesis of PANI doped with graphene oxide quantum dots via oligomer-initiated controlled polymerization in aqueous medium. The resulting composite material has exhibited a marked enhancement in electrochemical performance, which is attributed to the synergistic effects arising from the integration of the two components. This innovative approach has demonstrated the potential for achieving improved energy storage properties in advanced materials, paving the way for future applications in the fields of energy storage.

The present thesis is composed of four chapters. **Chapter 1** presents the introduction and forewords in the field of PANI hydrogel and carbon/PANI nanostructured materials. **Chapter 2** presents overall outlook and discussion on the role of oligoanilines in structural and physical properties of PANI. **Chapter 3** presents a study regarding emulsion polymerization of PANI in presence of DNNDSA in aqueous medium under low temperature. The morphological investigation revealed fibrillar network through FESEM and HRTEM studies. Through rheological assessment it was at 10˚C revealed that storage modulus G' and loss modulus G" are invariant with frequency sweep. Moreover at 10˚C, G' is greater than G", which indicates

gel formation. Introduction of AgNPs in hydrogel matrix results in marked increase of specific capacitance from 1100 F/g to 1350 F/g. Also, there is 4 times increase of photocurrent compared to pristine PANI gel. **Chapter 4** presents construction of 3D interconnected controlled nanostructure of pyrolyzed graphene and GOQD-doped PANI as electrode for electrochemical capacitors. Electrochemical performance suggests that controlled nanostructure is better performing electrode material than uncontrolled composite product. **Chapter 5** presents the summary of the thesis work and future prospects of the developed approaches for future design of multifuctional materials.

Chapter 2

Pivotal Role of Oligoanilines as Regulator of Polyaniline Chain Growth, Helicity and Overall Morphology

Introduction: Polyaniline (PANI) has received significant attention as conductive polymer owing to its simple and cost effective method of synthesis, light weight, environmentally benign nature etc.[6] Furthermore, it offers many attractive features such as high conductivity, availability in different oxidation states, doping-dedoping using simple acid/base chemistry etc. Nanostructured PANI has been found to be even more impactful as single material or as component in composites. The mechanism behind oxidative polymerization of aniline is well researched and it has been found that supramolecular organization of the oligoanilines produced during aniline polymerization, dictates the fate of final PANI chains.[6,15]Thus, a significant degree of control over the PANI chain lengths, helicity or their morphology may be exercised by controlling the structure as well as number of oligomers via controlling the polymerization parameters or by externally added oligomers of desired structure. Therefore, knowledge regarding the structure and reactivity of the oligoanilines is essential. Besides generating potential polymeric chains of various utility, the oligomers themselves have been reported to be pretty effective in various similar applications. There are numerous reports and many reviews which explore the synthesis and applications of PANI chains and the role of oligoanilines.

Mechanism of polymerization of polyaniline: Polymerization of aniline is generally done by oxidative polymerization method using ammonium peroxodisulfate (APS) in aqueous acidic medium.[1] The proposed mechanism for oxidation of aniline to PANI along with structures of pernigraniline and emaraldine salt forms are presented in **Scheme 2 (a&b)**.[6,14]

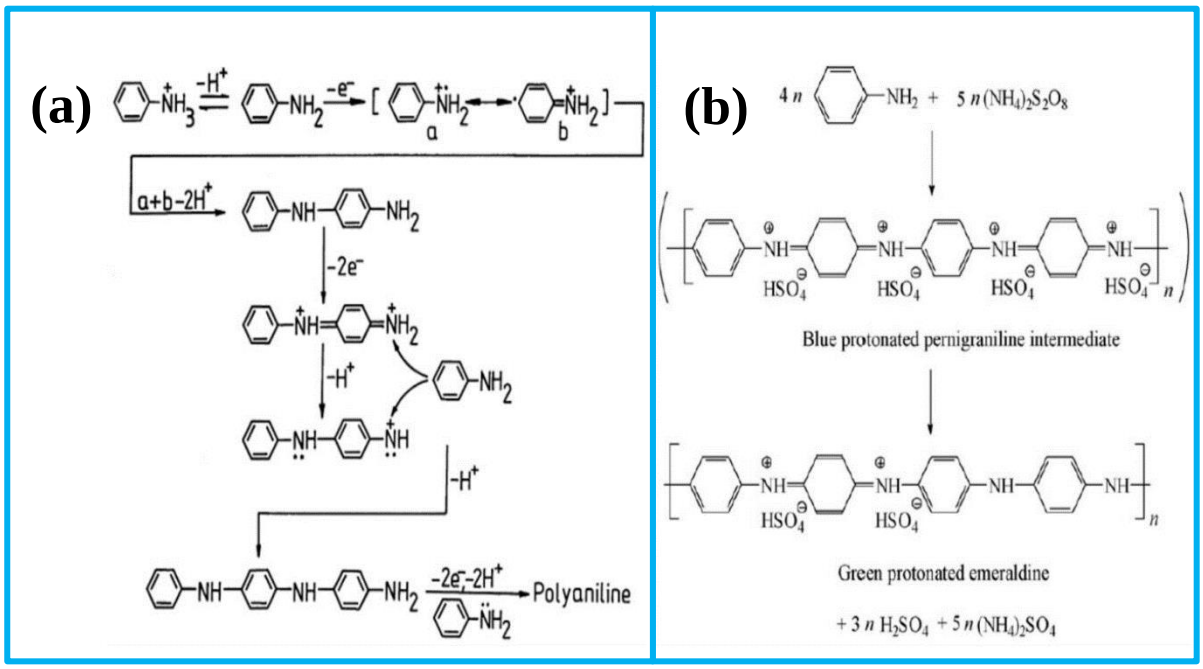

Scheme 1. *Mechanism of aniline polymerization (Reprinted from ref.6, 14)*

Revisiting the mechanism of chemical oxidative polymerization of aniline shows significantly higher oxidation potential (~0.9 V) is required for conversion of aniline to para aminodiphenylamine (dimer). However, it decreases sharply to ~0.4 V during conversion to trimeric [N-(4′-aminophenyl)-N′ phenyl-1,4-quinonediimine] from the dimer and it decreases further during conversion to tetramers or higher oligomers. Accordingly, aniline polymerization shows a long induction period , during which these oligomers are formed and subsequently much faster polymerization occurs.[14,23]

Role of oligoaniline in determining structural properties of polyaniline:

The foregoing discussion makes it apparent that use of externally added oligoanilines should be favorable for having control both over the chain length as well as morphology of the synthesized PANI. Accordingly, addition of *p*-phenylenediamine or semidine etc. reportedly helped faster generation of nucleates and the modified nucleates formed in presence of these additives stacked favorably to generate nanofibers.[6] Among oligomers, the aniline trimers

containing a phenazine moiety are important. They will be called nucleates, and although their detailed chemical structure is still open to discussion, they do exhibit some specific proper ties: (1) they have a relatively flat molecular structure and are able to produce one-dimensional stacks stabilized by–interactions; (2) they are hydrophobic and their solubility in water is low; (3) and they are able to adsorb on various surfaces in contact with the reaction mixture, preferably on hydrophobic surfaces. Depending on the type of the nucleates organization, the subsequent PANI growth can produce various morphologies: granules, nanofibers and, in combination with a template, nanotubes. (**Figure 2.1)** Other structures require the presence of a template interface, and they include thin films and coatings, colloidal nanoparticles, and more complex structures, such as nanobrushes or hairy spheres.[6]

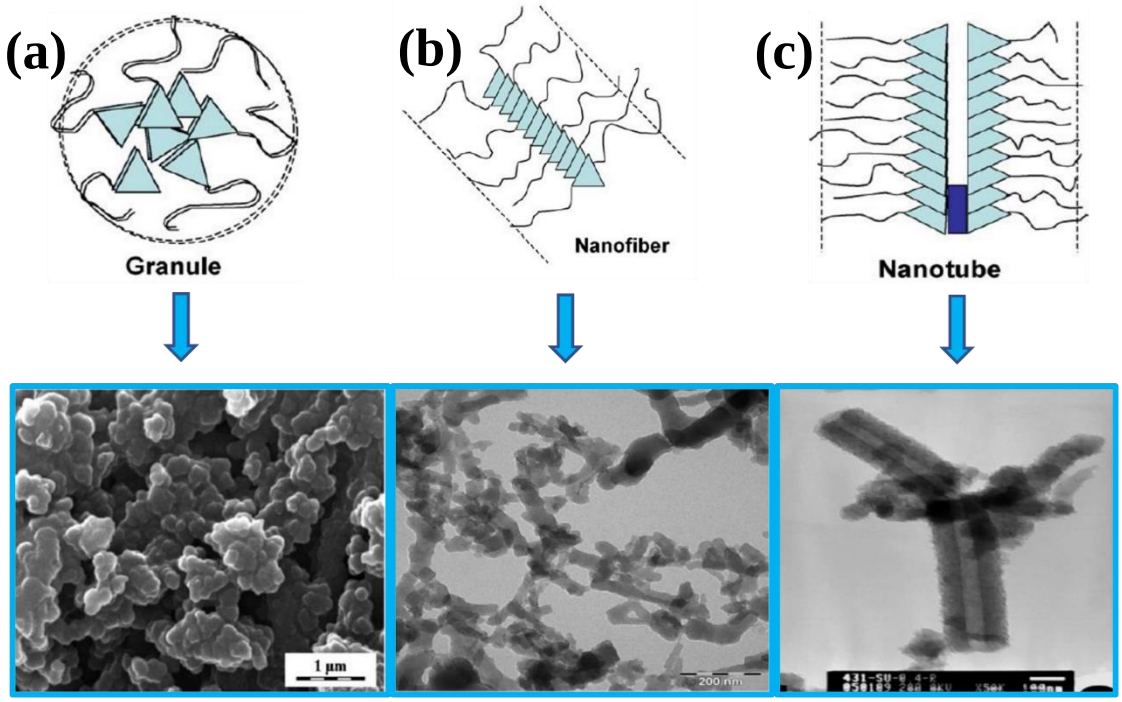

Figure 2.1. *Possible aggregation of oligoaniline nucleates to result different PANI nanostructures.* [6]

Now, length of the PANI chains and their nano structured morphology has been the key features in respect of the performance of the PANI electrodes in supercapacitors or battery applications. The literature reports show both covalent as well as non-covalent connection of PANI chains

on carbon materials for the preparation of such hybrid materials. However, in order to ensure better cohesion between the components it is apparent to have covalent connection between them. There are several reports where covalent connection of the PANI chains from the carbon nano materials have been accomplished by initiating the growth of the PANI chains from the aniline moieties tethered on the carbon nano material surfaces.[27-31] However, undeniably under these conditions, the threat of uncontrolled PANI chain generation due to competitive homogeneous nucleation in the polymerization bulk remains. This may arise as a genuine problem during scaling up of these methods of syntheses. In order to alleviate this, Chatterjee *et.al.* adopted a new strategy where a trimer of aniline N,N'-bis(4'-aminophenyl)-1,4-quinonediimine (APQD) was anchored on the carbon nanodot surface and then oxidative polymerization of aniline in dilute acid medium at low temperature was carried out.[5] The primary advantage of this method is the requirement of lower oxidative potential of this trimeric moiety compared to monomeric aniline which ensured faster growth of the PANI chains from them suppressing the homogeneous nucleation mechanism in the polymerization bulk. In this regard, in another report the same research group demonstrated the distinct effect of covalently attached APQD moieties in controlling synthesized PANI morphology from the GO sheet surfaces and the effect of heterogeneous catalysis of the insoluble GO sheets.[24]

Role of oligomers in determining helicity of polyaniline chains:

Chiral PANI has been synthesized in presence of chiral dopant, enzyme-catalyzed method, protein-guided biosynthesis, template-guided method *etc*.[32-34] Interestingly, simple protonation-deprotonation events are responsible behind doping-dedoping phenomenon of PANI therefore, induction of chirality in PANI chain have been achieved only by doping with chiral acids. However, chiral PANI synthesized in this route have low chirality which is a major bottleneck during their applications as chiral detectors. This drawback has been alleviated well by oligomer initiated polymerization of aniline where much improved chirality along with

appreciable enantioselectivity has resulted.[35] Aniline polymerization has typically slow reaction rate during the formation of dimer but reaction rate increases with subsequent formation of higher oligomers. In order to accelerate the rate of polymerization aniline oligomers were used where the oligomers act as 'seeds' for the growth of chiral PANI chains. The mirror image like CD spectra (**Figure 13a**) of enantiomeric PANI nanofibers doped by (+) CSA and (-) CSA indicated high degree of enantioselectivity of the reaction.

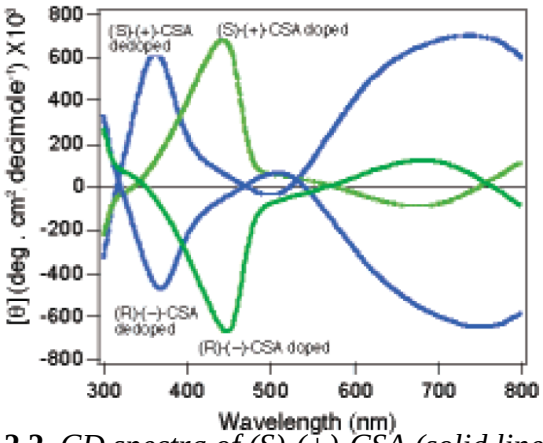

Figure 2.2. *CD spectra of (S)-(+)-CSA (solid line) and (R)-(-)-CSA (dotted line).*[35]

Chapter 3

Polyaniline-(dinonylnapthyl disulphonic acid) hydrogel showing enhanced supercapacitor and photo-current performance by in situ growth of AgNPs

Introduction: The conducting polymer gels exhibit overwhelming potential to develop flexible electronic devices for their 3D network structure, high conductivity, large pore volume, excellent solid-ligand interface, high surface area, and excellent optoelectronic properties.[36-38] PANI gels can be produced by various ways e.g., using phytic acid, folic acid as dopant cum gelator, surfactants like dinonyl napthyl sulphonic acid (DNNSA) and dinonylnapthyl disulphonic acid (DNNDSA), camphor sulphonic acid etc. mixed in the formic acid medium etc.[39]

In this article we describe the emulsion polymerization of aniline in presence of DNNDSA surfactant in water with APS initiator at 5ºC. In-situ growth of AgNPs in the same system exhibits increase of specific capacitance to 1350 F/g at the same current density at an optimum concentration of 1 % (W/V) $AgNO_3$ solution (PDAg1.2) taken during in-situ polymerization. Due to synergistic interaction between PANI polaronic bands and silver plasmon bands very good photocurrent and stable photocurrent switching is noticed.

Experimental details

PANI-DNNDSA (PD) gel:

The synthesis of PANI-DNNDSA gel was carried out in a 200 ml reactor vessel. 40 ml deionized water (Millipore) was taken in a temperature-controlled reaction vessel and it was kept at 5 ◦C. 1.32 g dinonylnapthyl disulphonic acid (DNNDSA) (Nacura-155, 45 wt% iso-butanol) dissolved in 10 ml water was added to it. Thereafter, 0.6 ml aniline was added to it drop wise. It was allowed to stir for 45 min creating a milky white emulsion. Cold ammonium persulfate (1.8 g in 5 ml water) was then added to it drop wise for a period of 30 min. During addition, it was observed that the milky white colour has changed to brown colour. The mixture was allowed to stir for 24 h maintaining the temperature at 5 ◦C while a deep green colour gel was formed. The gel thus formed was centrifuged, the precipitate was dispersed in ethanol, poured in a petri dish and was evaporated to dryness in a pool of air at 60 ◦C.

PANI-DNNDSA-Ag (PDAg) gels

The synthesis of PANI-DNNDSA-Ag gels were carried out in a similar fashion in 200 ml reactor vessel. Here before addition of APS, different volume (0.5, 1.0 and 1.5 ml) of AgNO3 solution (5.88 ×10 2 M) in water **(Table 3.1)** were added and similarly polymerized with APS solution. The gel formed was collected in the same process as mentioned above. The structure

of PANI-DNNDSA-Ag gels made by emulsion polymerization technique is presented in **Scheme 3.1.**

Table 3.1. Emulsion polymerization of PANI in presence of DNNDSA and its Ag nanocomposites

Sample	DNNDSA (g)	Aniline (mL)	$AgNO_3$ (mL)	APS (g)	Water (mL)	Atomic % of Ag from EDX
PD	1.32	0.6	-	1.8	40	-
PDAg0.6	1.32	0.6	0.5	1.8	40	0.57
PDAg1.2	1.32	0.6	1.0	1.8	40	1.23
PDAg1.6	1.32	0.6	1.5	1.8	40	1.56

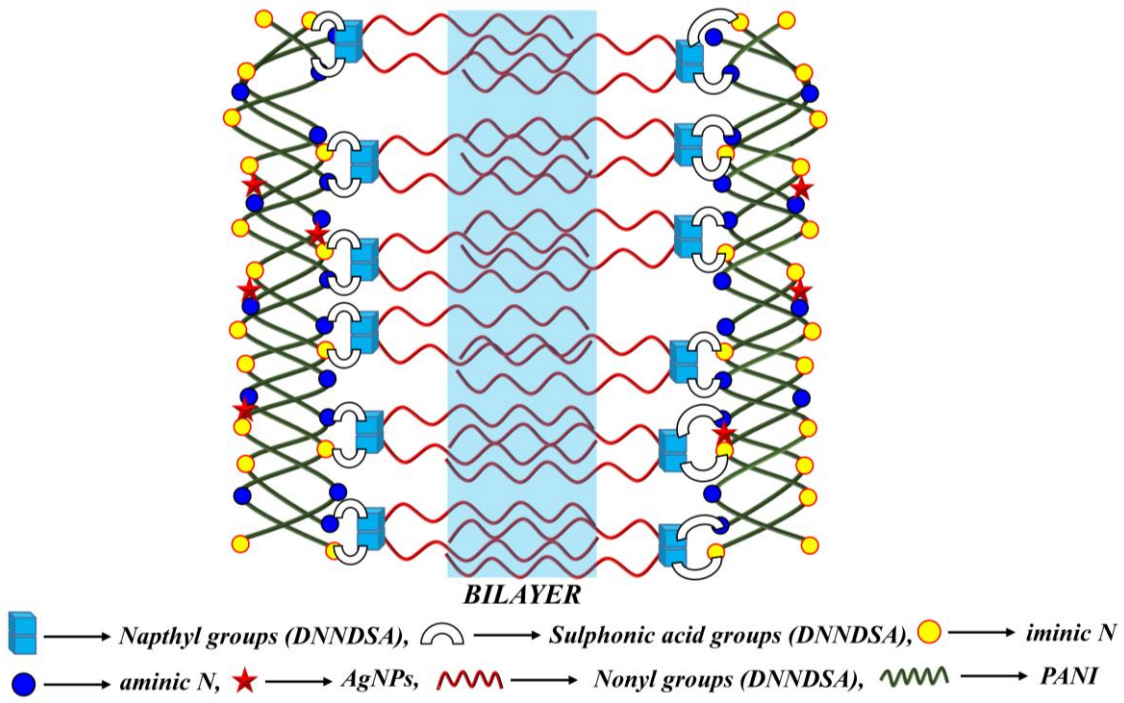

Scheme 3.1. Schematic presentation of the lamella model for a portion of polymer (PANI)-Surfactant (DNNDSA)- Nanoparticle (Ag) system in aqueous medium at 30ºC.

Results and discussions:

The FESEM morphology of the PD and PDAg systems (Fig. 3.1a-d) clearly reveal three dimensional (3D) fibrillar network morphology, characteristic of gel structure. In the Fig. 3.1(b -d) the AgNPs, are present as evident from the white spots on fibre surface of 3D network. From the HRTEM images 3D fibrillar network structure is clearly noticed for the PD system (Fig. 3.2a) and the presence of AgNPs are clearly noticed as black spots on the fibre surface in the Fig. 3.2(b-d) for PDAg0.6, PDAg1.2 and PDAg 1.6 samples, respectively. Here the density of AgNPs increases from PDAg0.6 to PDAg1.6 samples due to increased $AgNO_3$ concentration taken during preparation of the composites.

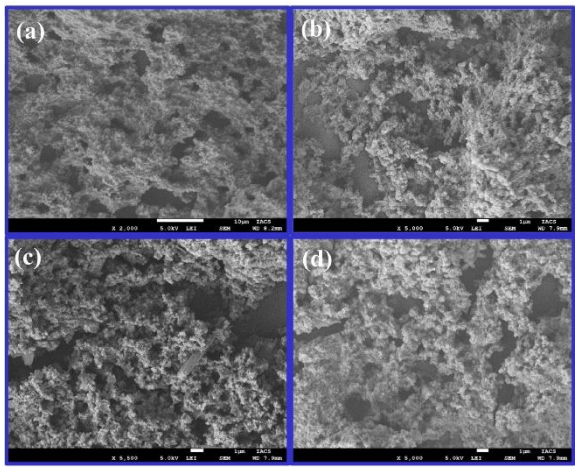

Fig.3.1. FESEM images of (a) PD, (b) PDAg0.6, (c) PDAg1.2 and (d) PDAg1.6.

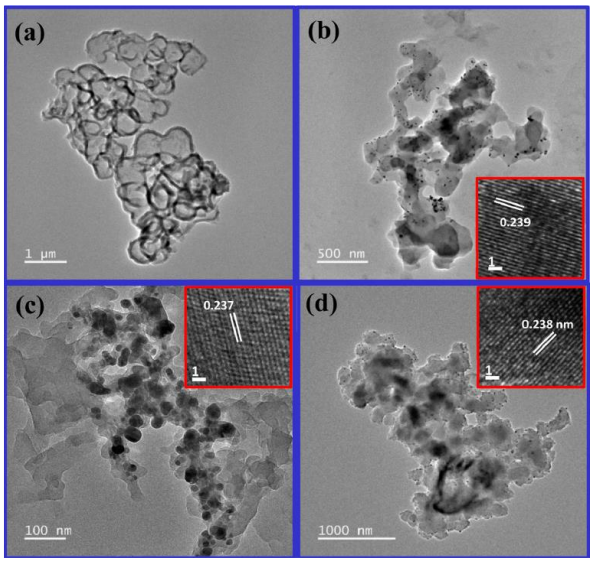

Fig.3.2. HRTEM images of (a) PD, (b) PDAg0.6, (c) PDAg1.2 and (d) PDAg1.6.

In **Fig. 3.3** IR data has been represented.

In **Fig. 3.4** UV-vis spectra is presented.

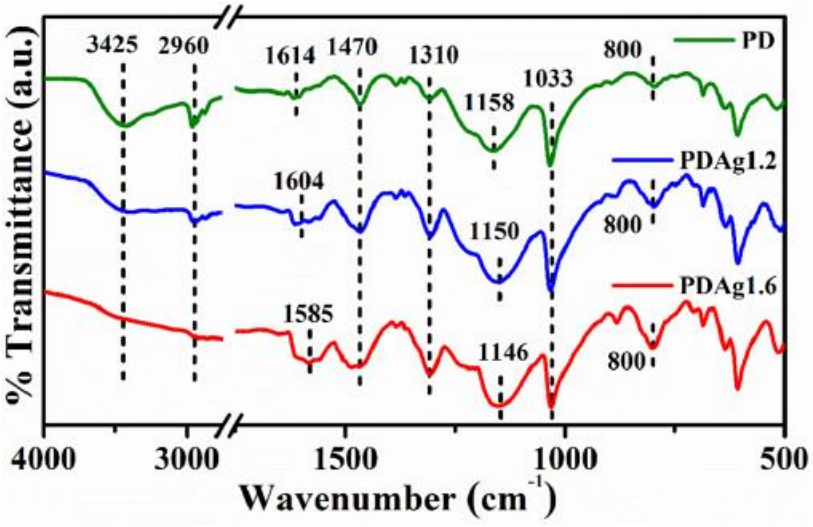

Fig.3.3. FT-IR spectra of PD, PDAg1.2 and PDAg1.6.

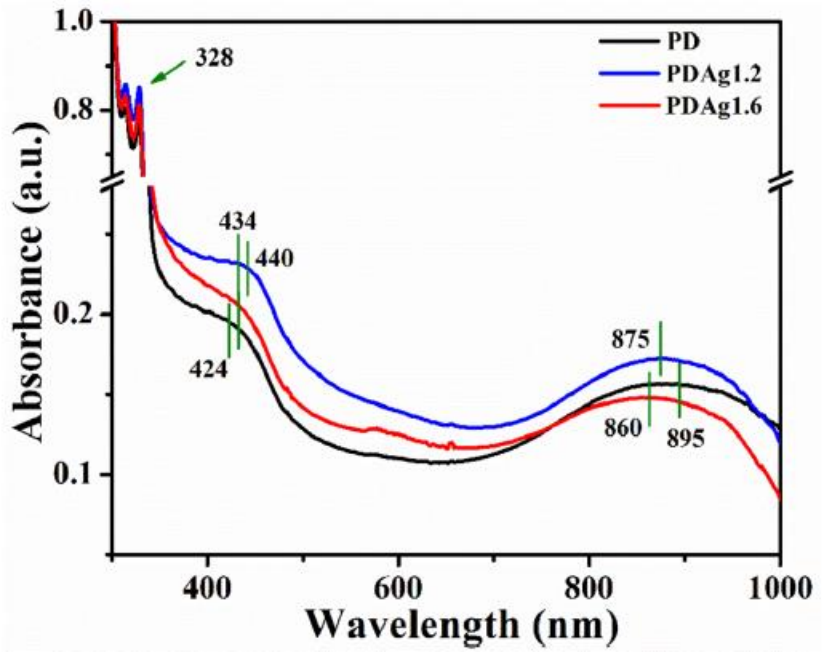

Fig.3.4. UV-vis spectra of PD, PDAg1.2 and PDAg1.6.

The X-ray diffraction pattern of PD and PDAg gel composites are presented in **Fig. 3.5** and it is evident that pure PD xerogel has diffraction peaks at 2θ = 3.63, 5.45, 5.93, 10. 0, 10.9,14.11, 16.42, 20.07 and 24.75. In the PDAg systems apart from those of PANI peaks some new peaks of AgNPs appear at 2θ = 27.97, 32.33, 38.21, 46.0, and 77.17 ◦ . The intensities of the new peaks gradually increase with increase of $AgNO_3$ concentration in the hybrids indicating increased AgNP formation.

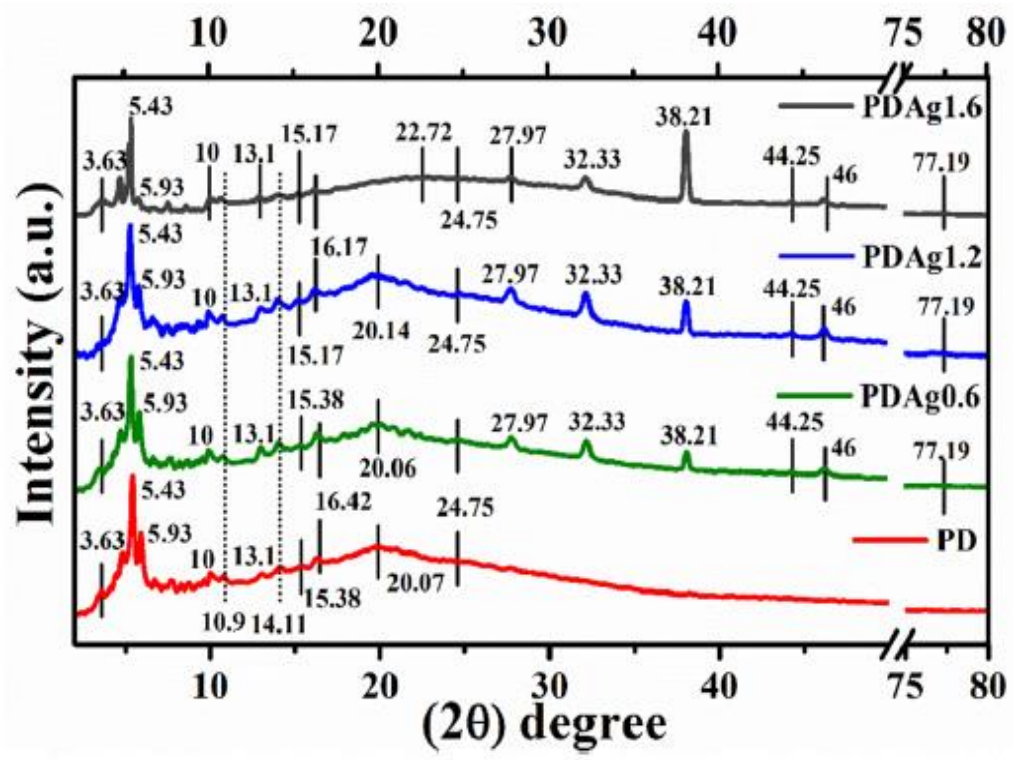

Fig.3.5. XRD analysis of all hydrogels

The formation of AgNPs in the DP gel is substantiated from the XPS study and the XPS spectra of PDAg1.6 sample is presented in **Fig. 3.6** where the binding energy peaks of different elements present in the sample are shown. In the survey scan spectrum, the XPS signals at 169.1 and 232 eV are for binding energies of electrons at S 2p states, respectively; C 1s and S 2s signal appears at 284 eV; the signals at 368 and 376 eV stands for AgNP; binding energies of N1s and O1s electrons appear at 408 and 532 eV, respectively, indicating formation of PDAg hybrid gel. The characteristic binding energy levels of AgNPs in the XPS spectra are distinctly shown in **Fig.3.6b** at 368.3 and 374 eV for the $Ag3d_{5/2}$ $Ag3d_{3/2}$ and states, respectively. The N 1 s spectra of PANI can be decon voluted into four different peaks centred at 398.6, 399.5, 401.5, and 402.3 eV **(Fig. 3.6c)** which are associated with quinoid imine, benzenoid imine,

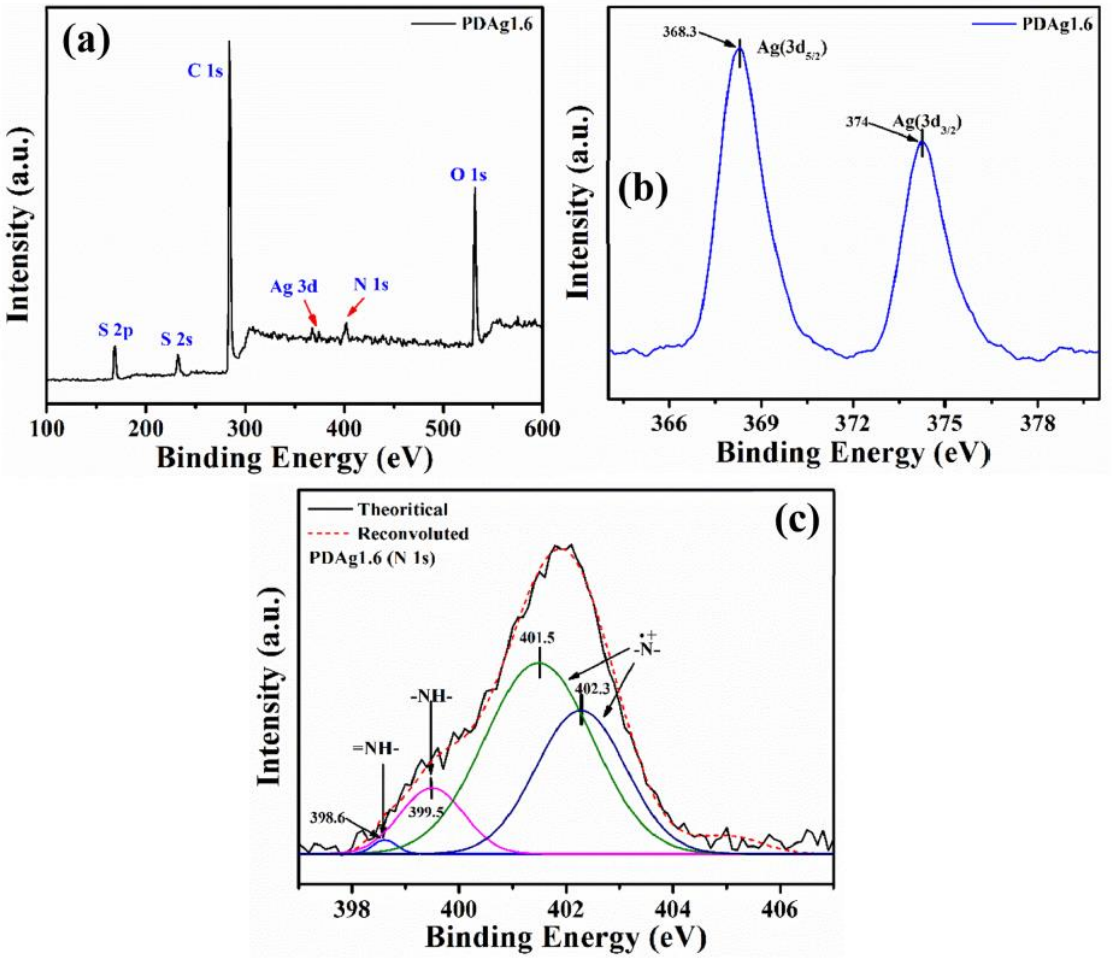

Fig.3.6. (a) XPS spectra (survey scan) obtained from PDAg1.6. (b) XPS core-level spectra of the Ag 3d regions and (c) Deconvoluted peak of N(1s) of PDAg1.6.

positively charged imine of bipolaron state, and protonated amine of polaron state, respectively.[40,41] Thus, the deconvoluted spectra of nitrogen atom clearly indicate the formation of radical cations indicating the presence of doped PANI by the surfactant DNNDSA. A ratio of the summation of area of deconvoluted peaks for polaron and bipolaron with the area of reconvoluted peak (dotted line) suggest about 85 % doping of nitrogen atoms of PANI by DNNDSA produced by emulsion polymerization technique.

The rheological property of PD hydrogel (W = 0.20) exhibits viscoelastic behaviour as evident from the plot of storage modulus (G and loss modulus (G ′) vs. angular frequency (ω PD ′)) **(Fig. 3.7 a-c)** made at ◦ C. It is evident from **Fig. 3.7a** that both G ′ 10 nonvariant with angular frequency (ω) and G ′ and G" are linear and G" values are higher than G' indicating viscoelastic nature of the gel. The gels are of robust nature as evident from high G ′ values (~10^4 Pa) and these excellent mechanical properties come from the formation of 3D fibrllar network of rigid PANI chains and the storage and dissipation of energy is easily facilitated from the covalent PANI chains.[42] Elasticity of gels are obtained from difference in magnitudes of G ′ and G ″ (G ′-G ″) and it increases in the order PD gel < PDAg1.6 gel < PDAg1.2 gel. **(Table 3.2)** This is quite interesting observation that PDAg1.2 gel shows maximum elasticity though PDAg1.6 has higher AgNP concentration indicating that PDAg1.2 has optimum AgNP concentration for synergistic interaction between AgNPs and PD gel network. It is also noted that PD gel shows stress at break 1.3 Pa, whereas PDAg1.2 and PDAg1.6 gels exhibit stress at break at 10.3 and 7.5 Pa, respectively. Thus, the presence of AgNps causes an increase in the stress at break because of the surface forces of AgNPs showing maximum for PDAg1.2 sample. At PDAg1.6 sample however the stress at break is lower from that of PDAg1.2 gel, probably due to agglomeration of AgNPs in the gel. Since PDAg1.2 exhibit highest elasticity, stress at break, storage modulus etc hence we expect good supercapacitor property in this system as the mechanical shock of charging-discharging process can be annihilated through the gel network.

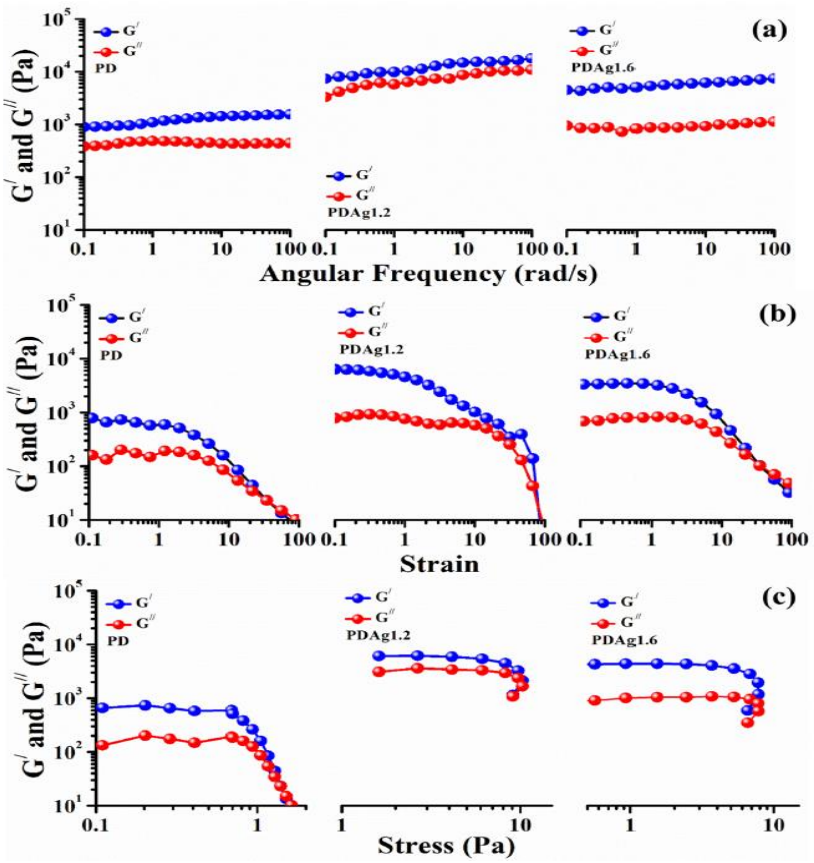

Fig.3.7. Plots of (a) storage modulus $G^{/}$ and loss modulus $G^{//}$ vs angular frequency (b) Plot of $G^{/}$ and $G^{//}$ vs oscillator strain at a constant frequency of 1 Hz and (c) Plot of $G^{/}$ and $G^{//}$ vs oscillator stress at a constant frequency of 1 Hz of the PD, PDAg1.0, and PDAg1.5 at 10°C.

Table 3.2- Comparison of rheological properties of PD, PDAg1.2 and PDAg1.6

Sample	Storage modulus (G') (Pa)	Loss modulus (G'') (Pa)	Elasticity (G'-G'') (Pa)	Stress at break (Pa)	Strain at break
PD	895	387	508	1.3	35
PDAg1.2	7403	3309	4094	10.3	67
PDAg1.6	4500	944	3556	7.5	35

In three electrode method the supercapacitor performance of PD and PDAg xerogels are monitored through CV, and galvanic charge-discharge (GCD) measurements in 1 M H_2SO_4 medium using the gel coated on glassy carbon electrode (GCE), Ag/AgCl reference electrode and Pt wire as counter-electrode.

In **Fig 3.8** the electrochemical performance of all the hydrogels in three electrode setups are shown. Here all the PD, PDAg0.6, PDAg1.2 and PDAg1.6 gels exhibit both double layer and pseudo capacitance characteristics in their CV profile and the area under the profile is found to be the highest for PDAg1.2 gel. At a scan rate of 5–100 mV/s, each gel exhibits electro chemical redox peaks within the range of 0.0– 0.8 V. This may be explained for the transformation of PANI from its leucoemeraldine / emeraldine and emeraldine / pernigraniline states, respectively.[8] The specific capacitance (C s) is calculated and the C s values of PD, PDAg0.6, PDAg1.2 and PDAg1.6 gels are 1100, 1160, 1350, 1220 F/g, respec tively, at a current density of 1 A/ g. Thus, AgNPs on fibrillar surface of PD enhances the supercapacitor performance and PDAg1.2 gel exhibit the highest specific capacitance indicating the contribution of AgNPs on 3 supercapacitor performance of PANI is optimum for addition of 1 % $AgNO_3$ concentration during the gel nanocomposite formation.

We prepared a 2-electrode solid state device by depositing PD and PDAg gels on carbon cloth, followed by drying and two such electrodes were sandwiched with PVA-H_2SO_4 gel electrolyte for measuring the CV curves **(Scheme 3.2)** with varied scan rates ranging from 5 to 100 mV/s to assess the electrochemical performance.

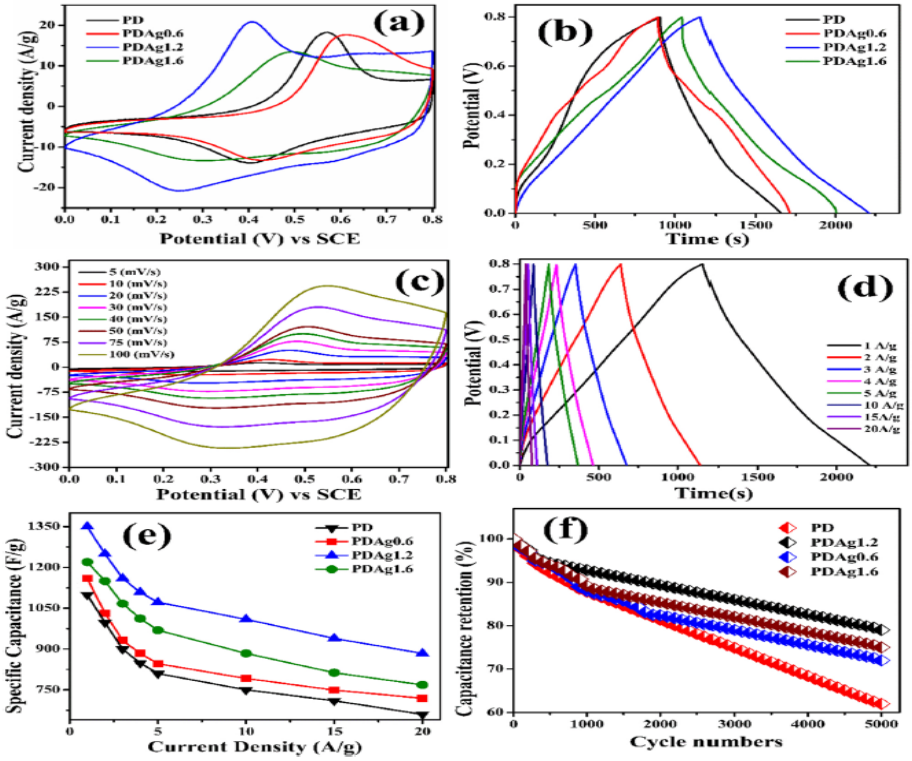

Fig.3.8. (a) CV curves of PD and all PDAg gels tested in 1(M) H_2SO_4 medium at scan rate of 5 mV/s; (b) GCD curves of PD and all the PDAg gels at 1 A/g current density (c) CV curve of PDAg1.2 gel at different scan rates (5–100 mV/s); (d) GCD profiles of PDAg1.2 at different current densities (1–20 A/g); (e) Variation of specific capacitance at different current densities (1–20 A/g); (f) Cyclic stability plot of PDAg1.2 and PD gels in three electrode setup at 10 A/g.

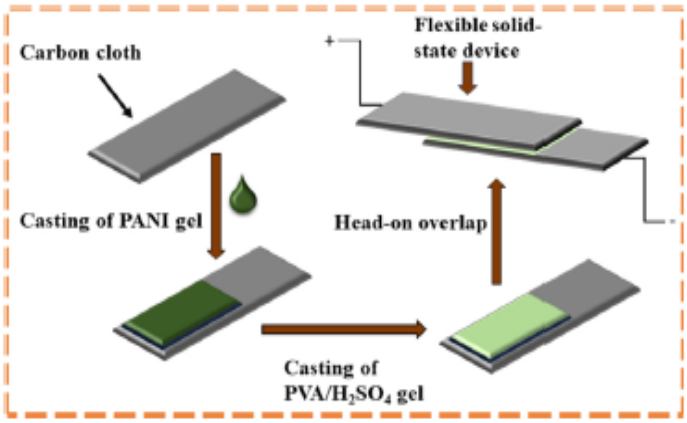

Scheme 3.2. Fabrication of solid state flexible two electrode CV measurement system using carbon cloth.

In **Fig 3.9** the electrochemical performance of the solid state device is shown. The CV curves show quasi rectangle shape with two peaks for redox transition of PANI and the curve area is maximum for the PDAg1.2 gel. From the discharge curves the specific capacitance (C s) values are calculated and the solid-state systems exhibit specific capacitance values of 500, 525, 646, 593 F/g for PD, PDAg0.6, PDAg1.2 and PDAg1.6, respectively. The flexible supercapacitor exhibits maximum energy density of 44 Wh/kg at a power density of 350.5 W/kg and it shows maximum power density of 7000 W/kg at energy density of 34.7 Wh/ kg. The 3D nanofibrillar structure of PDAg1.2 gel and synergistic interaction between PANI and AgNPs yield superior performance of power and energy densities for better ion transportation and curtailing of diffusion distance by absorbing the gel electrolyte thus acting as electrolyte reservoir.

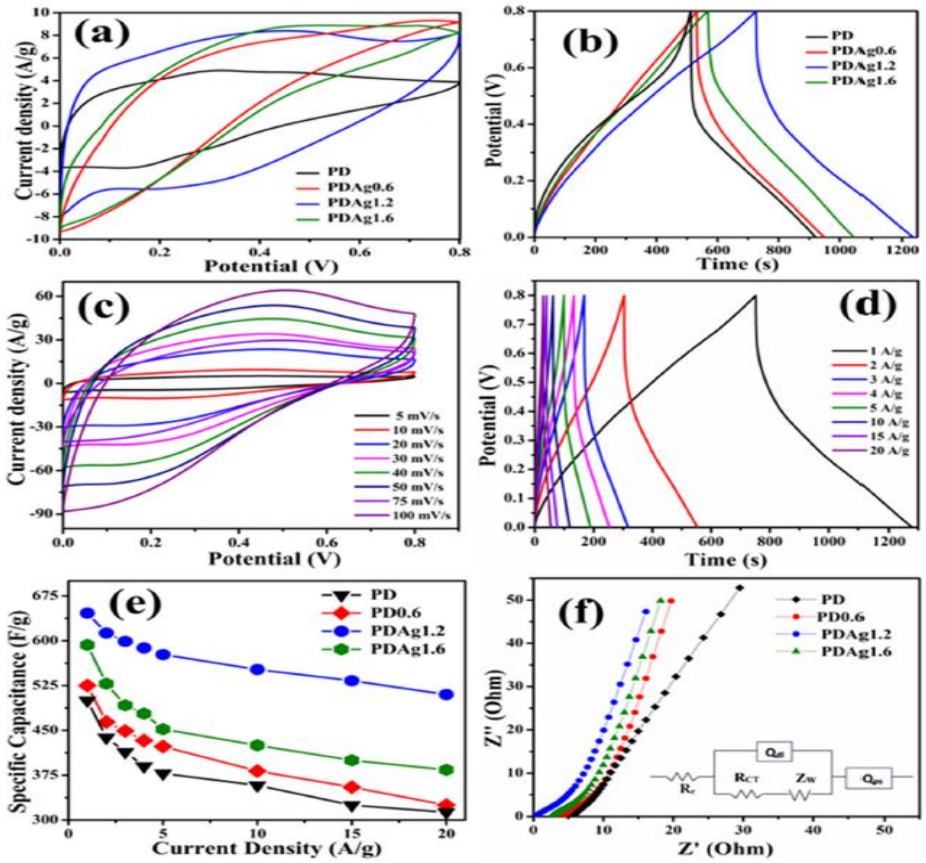

Fig.3.9. Electrochemical performance of solid state flexible supercapacitor: (a) CV curves of PD and all PDAg gels in two electrode method at 5 mV/s scan rate; (b) GCD profiles of PD and PDAg gels in two electrodes at 1 A/g current density; (c) CV curves of PDAg1.2 gels in different scan rates (5–100 mV/s) via two electrode method; (d) GCD curves of PDAg1.2 in different current densities (1–20 A/g); (e) Rate capability studies of PD and all PDAg gels in different discharge current densities (1–20 A/g); (f) Nyquist plots of PD and PDAg gels in 1–10 5 Table 5 Hz frequency range.

The current (I) – voltage (v) plots of PD, PDAg1.2 and PDAg1.6 xerogel **(Fig. 3.10a-c)** are shown under dark and white light illumination of 1 sun intensity. From the figures it is apparent that the photocurrent is higher in PDAg xerogels than that of PD xerogel **(Table 3.3)** showing photocurrent values of 0.49, 0.56, 2.1 and 1.84mA, for PD, PDAg0.6, PDAg1.2 and PDAg1.6 xerogels, respectively, measured at 5V bias for white light irradiation of 1 sun intensity. Thus, here about 4 times increase of photocurrent in the PDAg1.2 hybrid xerogel from that of PD xerogel is noticed.

Table 3.3. dc conductivity, I-V property in dark and light condition and photo current properties under white light illumination of 1 sun intensity.

Sample	dc Conductivity ($mScm^{-1}$)	*I-V* (mA)		Photo Current (mA)		
		Light	Dark	Photo Current (I_{on})	Dark Current (I_{off})	Gain (I_{on}/I_{off})
PD	0.09±0.02	0.49	0.31	0.49	0.41	1.20
PDAg0.5	0.10±0.02	0.56	0.40	0.57	0.55	1.03
PDAg1.0	0.17±0.03	2.10	1.08	2.17	1.96	1.10
PDAg1.5	0.13±0.03	1.84	0.90	1.87	1.77	1.06

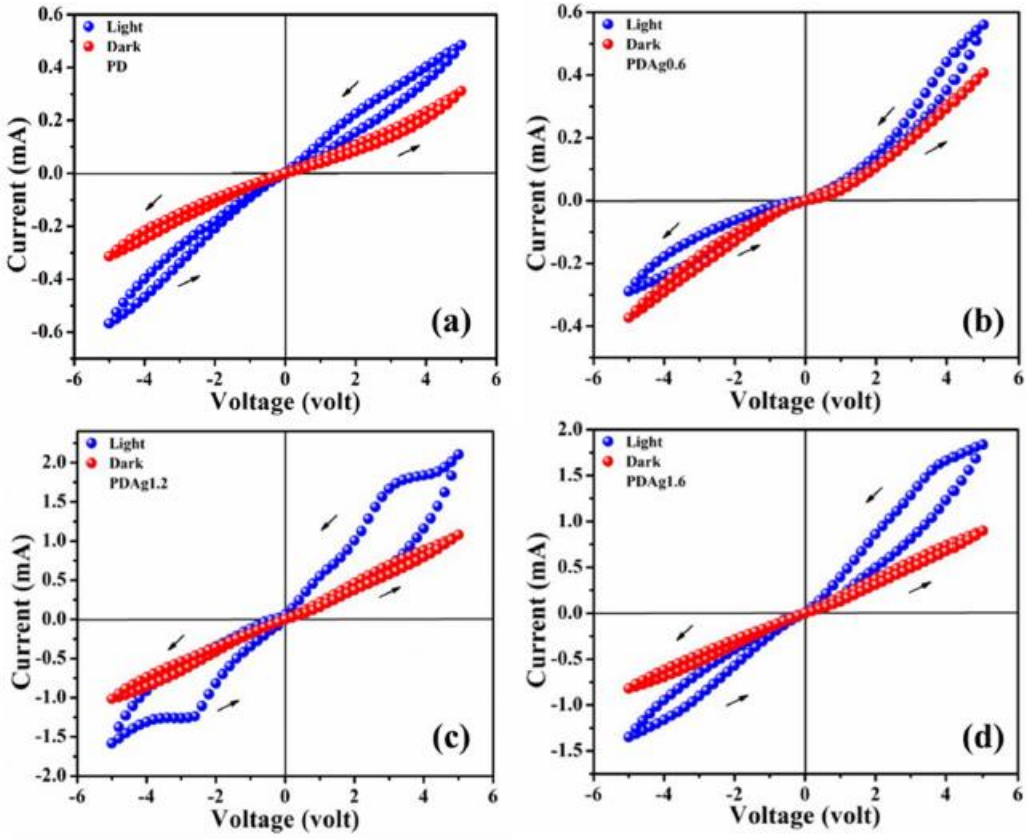

Fig.3.10. Photoresponse of (a) PD (b) PDAg0.6 (c) PDAg1.2 and (d) PDAg1.6. In both cases, the measurements were taken in the dark and under white-light illumination.

At dark condition the I-V plot shows purely semiconducting nature while at illuminated condition in the forward bias current increases linearly with voltage but at backward bias the current decreases with higher current value at each voltage than that of forward bias showing signature of memory effect. The difference between backward and forward current increases on growth of AgNPs in the PD gel and the gap is highest for PDAg1.2 gel indicating the highest memory among the other PDAg gels. The elec tronic memory in the PD gel may be attributed to storing of photo electrons on the napthyl rings of PANI-DNNDSA lamella, however, in PDAg gels the photoelectrons become also stored on the surfaces of AgNPs showing highest memory in PDAg1.2 gel. Probably a uniform dispersion and synergistic interaction of AgNPs in the PD gel matrix is the cause of highest photo-memory in the PDAg1.2 gel. This type of photocurrent memory in PDAg system is a new observation and might be useful in different photoelectronic devices.

Chapter 3

Preparation of Highly Efficient 3D Network Structured Pyrolyzed Graphene Oxide/Polyaniline Composite Electrode for Flexible Supercapacitor

Introduction:

In the previous chapter, remarkable improvement of energy storage performance was obtained by incorporation of AgNPs inside PANI hydrogel which was primarily due to pseudocapacitance. However, to inhibit the volume degradation of PANI during repetitive charge-discharge cycles integration of carbon nanomaterials with PANI is important. [7] In this process a nanocomposite with enhanced cycle life and rate capability will be obtained. Hence in order to extract best synergy between pseudocapacitor and EDLC components, controlled growth of PANI over 2D-graphene surface is envisaged. In this chapter, 2D graphene obtained from pyrolysis of graphene oxide was integrated with GOQD-doped PANI nanotubes via oligomer-initiated controlled polymerization. The synthesized composite exhibited significantly improved performance through the synergistic effect of these two components.

Results and discussions:

The FESEM image of p-GO sheets exhibits randomly distributed wrinkled sheets of different sizes mostly greater than 2μm upto 8 μm. A significant change in surface morphology is observed in case of PGQT (where the mixture of p-GO, GQD, APQD and aniline has been thoroughly sonicated under similar condition of PGQTP50 but without addition of APS). The morphology of p-GO sheets changes from wrinkled to flat surface which indicated significant interaction between APQD/GQD composite and p-GO sheets. Moreover, cross-section image of PGQT shows that APQD-GQD particles are present in between p-GO sheets. In case of PGQTP50 3D-interconnected network morphology of relatively shorter p-GO and PANI nanotubes are observed. In this regard, the PANI nanotubes restricts the stacking of p-GO sheets, thus forming a porous structure which facilitates ion movement through the nanostructure. (**Fig.4.1)**

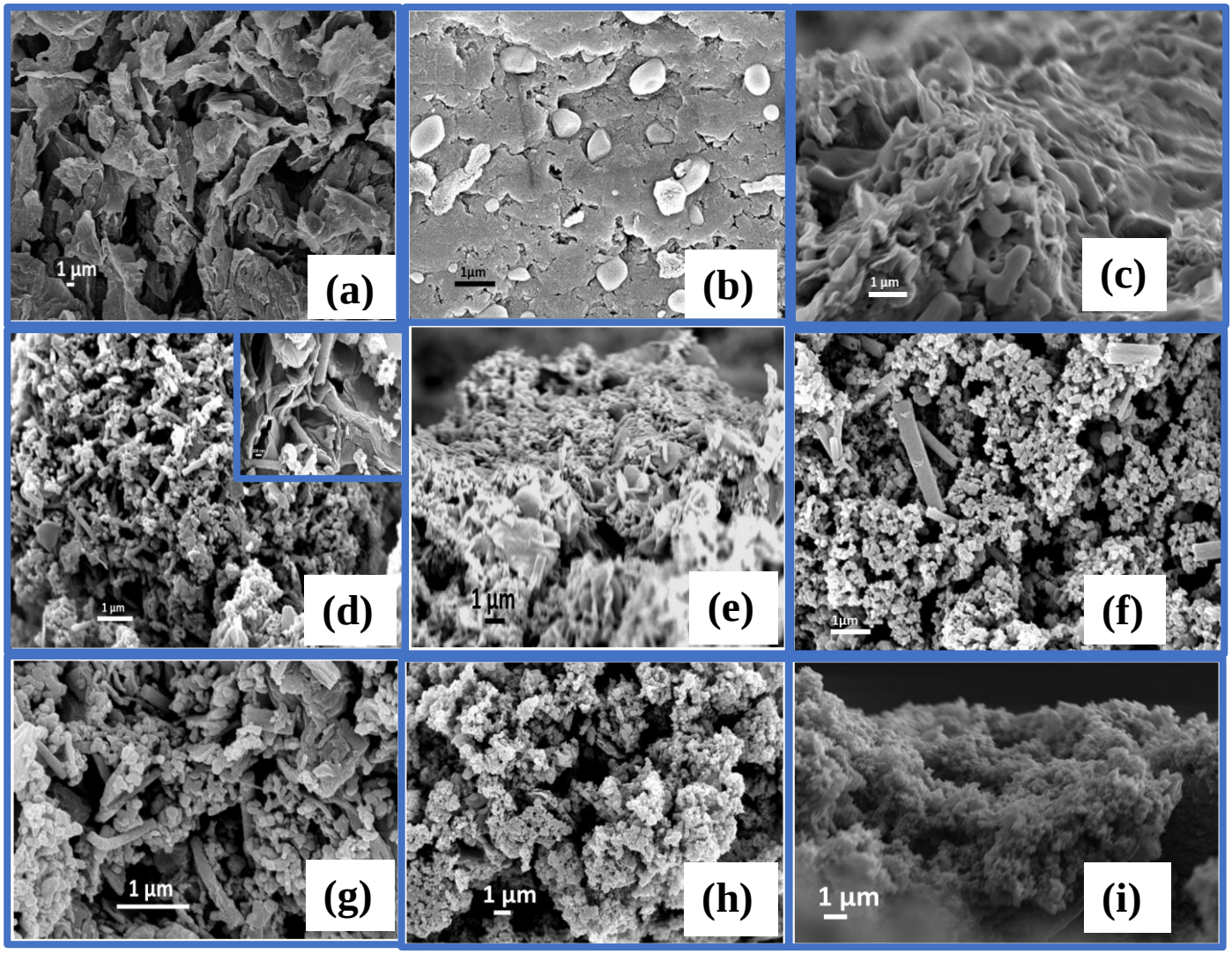

Figure 4.1: FESEM images of (a) p-GO, (b) PGQT, (c) cross-section image of PGQT, (d) PGQTP50, (e) cross-section image of PGQTP50, (f) PGTP50, (g)PGQP50, (h) PGP50, (i) cross-section image of PGP50; inset in (d) showing the expanded view.

FT-IR spectra exhibited that after polymerization of aniline in all of the samples PGQTP50, PGQP50, PTP50 and PP50 the signal corresponding to the (N-H) stretching vibration in the range of 3410 cm^{-1} is almost invisible due to PANI formation. The N_2 adsorption-desorption BET analysis of GO and p-GO shows sp. The CV analysis of PGQTP50 shows a rectangular plot with a pair of broad peaks at ~0.21 V and 0.48 V corresponding to the oxidation of semi-conducting leucoemeraldine to emeraldine and emeraldine to pernigarniline forms of PANI respectively.[24] **(Fig.4.2a)** Other composite sample show similar plots as PGQTP50 however, the area under the curve in each case is lower than PGQTP50. **(Fig.4.2b)** The nonlinearity observed in the GCD discharge profile for all of the composite samples including PGQTP50 suggests occurrence of PANI pseudocapacitance and the greater duration of discharge for PGQTP50 indicates it's highest sp. Capacitance value. **(Fig.4.2 c&d)**

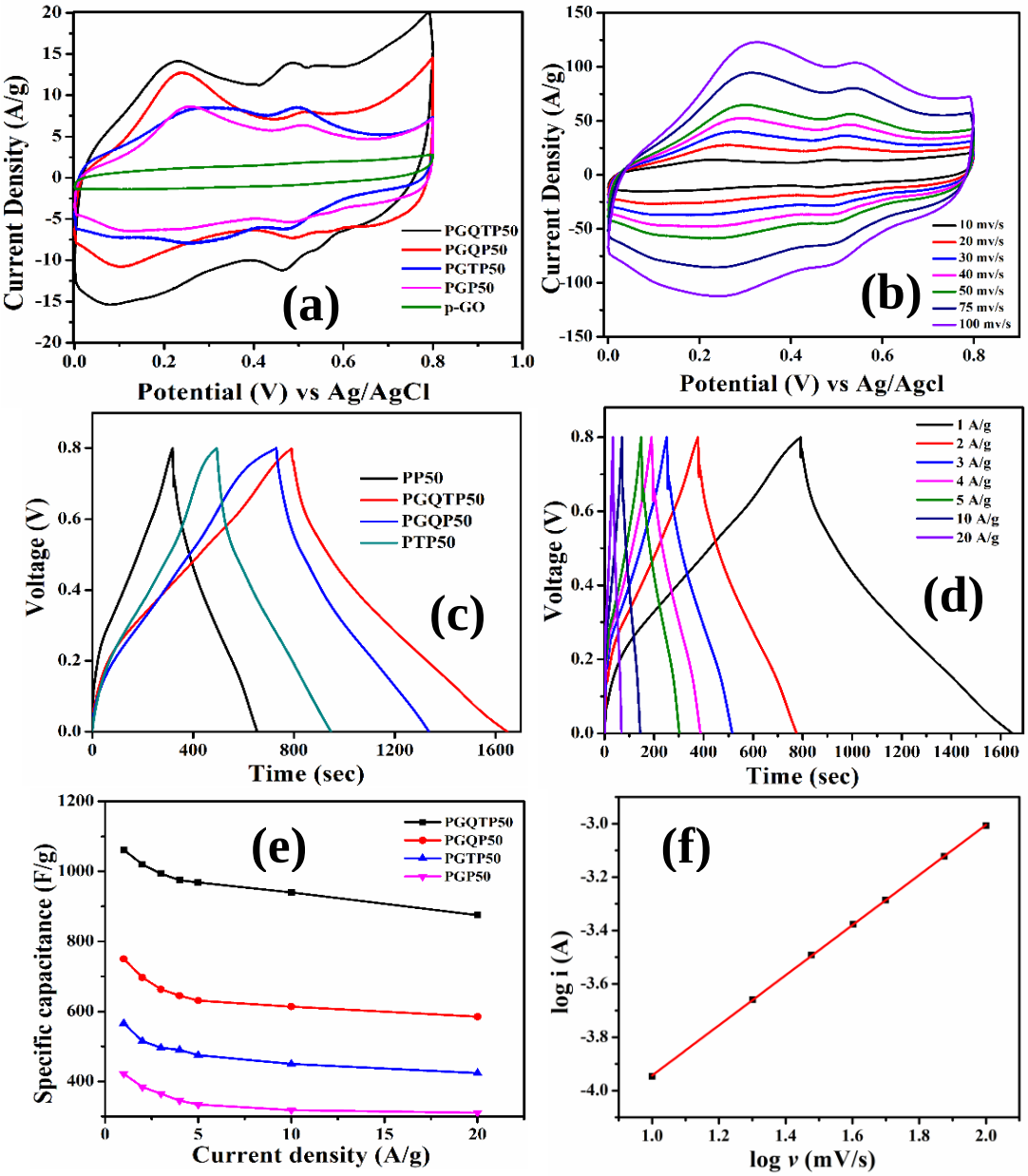

Figure 4.2: (a) CV curves of p-GO and all nanocomposites tested in 1(M) H_2SO_4 medium at scan rate of 10 mV/s; (b) GCD curves of all nanocomposites at 1 A/g current density (c) CV curve of PGQTP50 at different scan rates (10–100 mV/s); (d) GCD profiles of PGQTP50 at different current densities (1–20 A/g); (e) Variation of specific capacitance at different current densities (1–20 A/g); (f) logi vs logν plot for PGQTP50.

Now in order to find out the origin of the remarkably high rate performance, an attempt is made to resolve the total sp. Capacitance of the composites to get the contribution of EDLC. This is obtained from the plot of galvanostatic charge vs frequency plot where dividing charge at $\nu=0$ and $\nu=\infty$ separately by the voltage range gives total maximum sp. Capacitance and double layer capacitance respectively.[43] Furthermore, fitting the current i(V) at a particular potential (V) with the scanning frequency (ν) according to the Power-law dependency $i(V)=a\nu^b$ results a

value of 0.91 for the component ‘b’. **(Fig.4.2f)** This also points out towards the principally capacitative nature of charge storage (as b~0.5 indiactes diffusion-controlled process and b~1 indicates capacitative process).

Chapter 5

Summary of research work and future objectives

The present thesis work successfully demonstrates preparation of nanostructured polyaniline-based electrode materials for supercapacitor applications. The prepared nanomaterials via oligomer-initiated polymerization and emulsion polymerization constructs an avenue of further research on these topics.

Graphene oxide, reduced graphene oxide, carbonized graphene oxide materials have been used as typical EDLC material in the field of supercapacitor. Reduced graphene oxide (rGO) with higher specific surface area has greater conductivity than graphene oxide.[19] In this regard, Ag-doped-DNNDSA/PANI hydrogel composite will be synthesized inside rGO sheets. The 3D interconnected network should be obtained, which will have greater specific capacitance, power density, energy density and cyclic stability compared to Ag-doped- DNNDSA/PANI electrode.

As one of the typical layered transition metal dichalcogenides, MoS_2 has analogous structure to graphite.[44] However the 2H-phase MoS_2 exhibits poor conductivity leading to poor cyclic stability. 1T-phase MoS_2, with different arrangement of atomic layers, exhibits superior conductivity (~ 10^5 times than 2H-phase MoS_2) compared to 2H-phase.

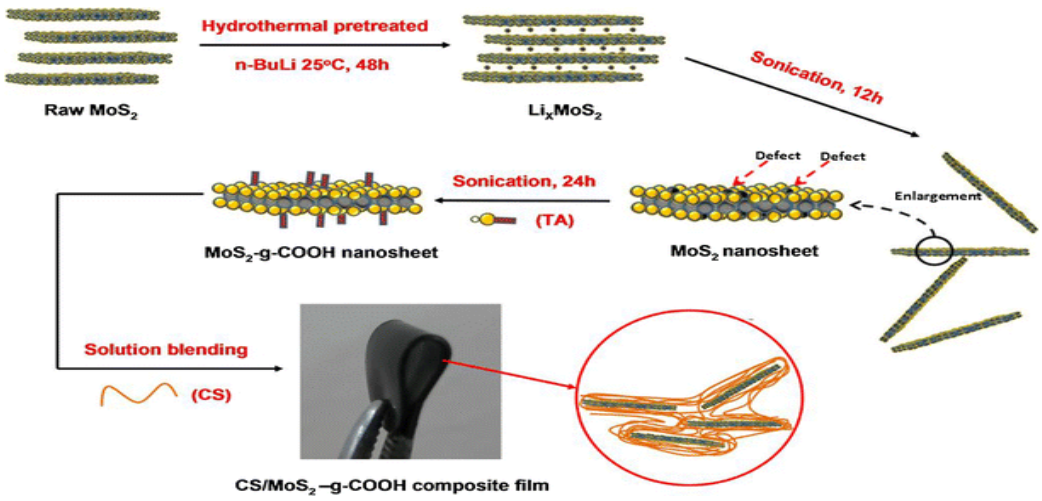

Scheme 5.1. Fabrication of MoS2–g COOH and preparation of CS/ MoS2–g–COOH composite films

Furthermore, 2DMoS2/PANI composite have been prepared for energy storage applications.[7,45] In this regard MoS_2 nanosheets will be covalently grafted with acidic functional group leading to MoS_2-COOH.[46] (**Scheme 5.1)**

Tetraaniline (TANI) is the tetramer of aniline which has better cyclic stability than PANI due to shorter chain length which can withstand mechanical shock during repetitive charge-discharge process.[47] In this situation, TANI will be grown inside the MoS2-COOH. TANI should be doped by acidic functionalities of MoS2-COOH which will give better synergistic interaction between MoS2 and TANI. Also replacing PANI with TANI will increase the cyclic stability. Therefore, integrating 1T-MoS2 and TANI will produce advanced electrochemical capacitor with high performance attributes.

Three-dimensional network structure of metal derivatives like oxides, sulphides etc. or metal organic framework (MOF) are having highly porous structure. This increased specific surface area of such porous network structure and possibilities of easier ion movement are advantageous for supercapacitor electrodes operating through *EDLC* mechanism.[48] However, poor conductivity of such network structure seriously limits their said applications. Wang et.al.[49] have reported MOF/PANI nano composite formation for introduction of improved conductivity. In this nano composite, large and randomly connected PANI chains wrap the framework structure and thus provide improved conductivity (**Scheme 5.2**).

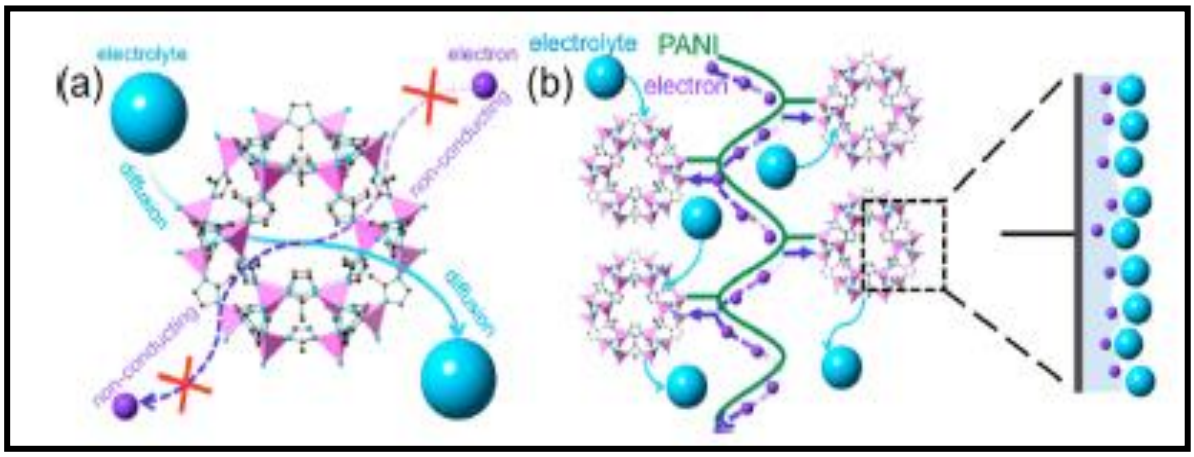

Scheme 5.2: Wrapping of MOF with conducting PANI chains[49]

A modified strategy may be put forward where GQD nano particles will be entered inside the pores of the MOF and then growth of TANI chains will be affected from them. This would generate a MOF based nano composite material with much improved conductivity. Hence a significant improvement in energy storage is expected.

References:

1. Z. Yu, M. McInnis, J. Calderon, S. Seal, L. Zhai and J. Thomas, *Nano Energy,* 2015, **11,** 611–620.
2. Thiyagarajan, M.; Samuelson, L. A.; Kumar, J.; Cholli, A. L. *J. Am. Chem. Soc.,* 2003, **125,** 11502-11503.
3. Z. Yu, L. Tetard and J. Thomas, *Energy Environ. Sci*., 2015, **8,** 702–730.
4. D. P. Chatterjee , A. K. Nandi. *J. Mater. Chem. A*., 2021, **9,** 15880-15918.
5. Z.-F. Li, H. Zhang, Q. Liu, Y. Liu, L. Stanciu and J. Xie, *Carbon*, 2014, **71,** 257–267.
6. J. Stejskal, I. Sapurina, M. Trchová. *Prog. Polym. Sci.,* 2010, **35,** 1420–1481.
7. D. P. Chatterjee, A. K. Nandi. *J. Mater. Chem. A.,* 2023, **11,** 12593-12642.
8. S. Das, R. Ghosh, D. Mandal, A.K. Nandi. *ACS Appl. Energy Mater.,* 2019, **2,** 6642.
9. L. Pan, G. Yu, D. Zhai, H.R. Lee, W. Zhao, N. Liu, H. Wang, B.C.-K. Tee, Y. Shi, Y. Cui, Z. Bao. *Proc. Natl. Acad. Sci. U. S. A*., 2012, **109,** 9287.
10. S. Das, P. Chakraborty, S. Mondal, A. Shit, A.K. Nandi. *ACS Appl. Mater. Interfaces.,* 2016, **8,** 28055.
11. T. Jana, A.K. Nandi. *Langmuir*., 2000, **16,** 3141.
12. T. Jana, A.K. Nandi. *Langmuir.,* 2001, **17,** 5768.
13. T. Jana, J. Chatterjee, A.K. Nandi. *Langmuir.* 2002, **18,** 5720–5727.
14. N. Gospodinova, L. Terlemezyan. *Prog. Polym. Sci.*, 1998, **23,** 1443–1484.
15. I. Sapurina, J Stejskal. *Polym Int*., 2008, **57,** 1295–325.
16. N. A. Kumar, H. J. Choi, Y. R. Shin, D. W. Chang, L. Dai, J. B. Baek. *ACS Nano.* 2012, **6,** 1715−1723.
17. Y. Liu, Y. Ma, S. Guang, F. Ke, H. Xu. *Carbon,* 2015, **83,** 79−89.
18. B. Zhao, P. Liu, Y. Jiang, D. Pan, H. Tao, J. Song, T. Fang, W.Xu. *J. Power. Sources.,* 2012, **198,** 423-427.
19. F. Du, D. Yu, L. Dai, S. Ganguli, V. Varshney and A. K. Roy, *Chem. Mater.,* 2011, **23,** 4810–4816.
20. F. Zeng, Y. Kuang, N. Zhang, Z. Huang, Y. Pan, Z. Hou, H. Zhou, C. Yan, O. G. Schimdt. *J. Power. Sources.,* 2014, **247,** 396-401.
21. S. Mondal, U. Rana and S. Malik, *Chem. Commun*., 2015, **51,** 12365–12368.
22. S. Zhang, L. Sui, H. Dong, W. He, L. Dong, L.Yu, *ACS Appl. Mater. Interfaces.,* 2018, **10,** 12983−1299.

23. C. Luo, H. Peng, L. Zhang, G-L. Lu, Y. Wang, and J. Travas-Sejdic, *Macromolecules*, 2011, **44,** 6899–6907.
24. T. Ghosh, R. Ghosh, U. Basak, S. Majumdar, R. Ball, D. Mandal, A. K. Nandi, D. P. Chatterjee. *J. Mater. Chem. A.,* 2018, **6,** 6476–6492.
25. T. Ghosh, U. Basak, P. Bairi, R. Ghosh, M. Pakhira, R. Ball, B. Biswas, D. P. Chatterjee. *ACS Appl. Nano Mater.,* 2020, **3,** 1693−1705.
26. S. Balasubramanium, A. Mohanty, S. K. Balasingam, S. J. Kim and A. Ramadoss, *Nano-Micro Lett.,* 2020, **12,** 85.
27. N. A. Kumar, H. J. Choi, Y. R. Shin, D. W. Chang, L. Dai, J. B. Baek. *ACS Nano.,* 2012, **6,** 1715−1723.
28. Z. F. Li, H. Zhang, Q. Liu, L. Yadong, L. Stanciu, J. Xie. *Carbon.* 2014, **71,** 257− 267.
29. Y. Liu, Y. Ma, S. Guang, F. Ke, H. Xu. *Carbon.* 2015, **83,** 79−89.
30. M. Kumar, K. Singh, S. K. Dhawan, K. Tharanikkarasu, J. S. Chung, B. S. Kong, E. J. Kim, S. H. Hur. *Chem. Eng. J*. 2013, **231,** 397−405.
31. Z. Gao, F. Wang, J. Chang, D. Wu, X. Wang, X. Wang, F. Xu, S. Gao, K. Jiang. *Electrochim. Acta*. 2014, **133,** 325− 334.
32. L. A. P. Kane-Maguire, G. G. Wallace. *Chem. Soc. Rev.* 2010, **39,** 2545–2576.
33. F. Zou, L. Xue, X. Yu, Y. Li, Y. Zhao, L. Lu, X. Huang, Y. Qu. *Colloids Surf. A Physicochem. Eng. Asp.* 2013, **429,** 38–43.
34. A. V. Caramyshev, V. M. Lobachov, D. V. Selivanov, E. V. Sheval, A. Kh. Vorobiev, O. N. Katasova, V. Y. Polyakov, A. A. Makarov and I. Y. Sakharov. *Biomacromolecules*, 2007, **8,** 2549-2555.
35. W. Li, H. L. Wang. *J. Am. Chem. Soc.*2004, **126,** 2278-2279.
36. N.K. Mahenderkar, Q. Chen, Y.-C. Liu, A.R. Duchild, S. Hofheins, E. Chason, J. A. Switzer, *Science*, 2017, **355,** 1203.
37. L. Hu, Y. Cui, *Energy Environ. Sci.*, 2012, **5,** 6423.
38. X. Wang, X. Lu, B. Liu, D. Chen, Y. Ton, G. Shen, Adv. Mater. 2014**, 26,** 4763.
39. P. J. Kinlen, J. Liu, Y. Ding, C. R. Graham, E. E. Remsen, *Macromolecules,* 1998, **31,** 1735–1744.
40. A. Choudhury. *Sensors and Actuators B*, **2009,** 138, 318–325.
41. M. M. Oliveira, E. G. Castro, C. D. Canestraro, D. Zanchet, D. Ugarte, L.S. Roman, A. J. G. Zarbin. *J. Phys. Chem. B*, **2006,** 110, 17063-17069.
42. P. Chakraborty, P. Bairi, B. Roy, A. K. Nandi. *ACS Appl. Mater. Interfaces.* **2014,** 6, 3615.

43. T. Brezesinski, J. Wang, J. Polleux, B. Dunn, S. H. Tolbert, *J. Am. Chem. Soc.*, **2009,** 131,1802.
44. R. Zeng, Z. Li, L. Li, Y. Li, J. Huang, Y. Xiao, K. Yuan, Y. Chen, *ACS Sustain.Chem. Eng.*2019, **7,** 11540-11549.
45. M. Kim, Y. K. Kim, J. Kim, SW. Cho, G. Lee, J.Jang, *RSC Adv.,* 2016, **6,** 27460-27465.
46. X.Yang, N. Meng, Y. Zhu, Y. Zhou, W. Nie, P. Chen, *J. Mater. Sci.,* 2016, **51,**1344–1353.
47. X. Chang, M. F. El-Kady, A. Huang, C-W. Lin, S. Aguilar, M. Anderson, J. Z. J. Zhu, and R. B. Kaner, *Adv. Funct. Mater.,* 2021, **31,** 2102397.
48. C. Km, J. Hm, P.Jh, Z. Yb, K. Jk, Y.Om, *ACS Nano,* 2014, **8,** 7451-7457.
49. L. Wanf, X. Feng, L. Ren, Q. Piao, J. Zhong, Y. Wang, H. Li, Y. Chen, B. Wang, *J. Am. Chem. Soc.* 2015, **137,** 4920−4923.

List of Publications:

1. **Arindam Das,** Sourav Bej, Nithun Ranjan Pandit, Priyabrata Banerjee and Biplab Biswas, *J. Mater. Chem. A***,** 2023, **11**, 6090-6128.
2. Udayan Basak [1], **Arindam Das [1]**, Soumya Maity, Dhruba P. Chatterjee, Arun K. Nandi, *Colloids Surf. A Physicochem. Eng. Asp.,* 2024, **685,** 133193. (**[1] = Equal contribution)**
3. Nithun Ranjan Pandit, Biplab Biswas, Sandip Paul, **Arindam Das,** Anjay Majhi, Sunny Goon, Prapti Priyam Handique, Arpita Gucchait, International Journal of Chemical and Environmental Sciences, 2022, **3,** 53-60.

Papers presented in International/National Conferences:

1. 'Carbonized Graphene Oxide/ GOQD-doped Polyaniline with Controlled Nanostructure as Electrodes for Improved Electrochemical Capacitors', **Poster** presented in one day national symposium on **Frontiers in chemistry: From fundamentals to application**; March 28, 2023 at **Presidency University, Kolkata.**
2. 'Pyrolyzed Graphene Oxide/ GOQD-doped polyaniline with controlled nanostructure as electrodes Improved Electrochemical Capacitors', **Poster** presented in **P. C. Ray memorial international conference on Contemporary ideas, innovations and**

initiatives in chemical sciences-2023; August 23-24, 2023 at **Presidency University, Kolkata.**

3. 'Polyaniline-(dinonylnapthyldisulphonic acid) hydrogel showing enhanced supercapacitor performance by in situ growth of AgNPs', **Poster,** presented in **International workshop on Functional polymers and its nanocomposites**; February 9-10, 2024 at **Rubber technology centre, IIT Kharagpur.**

Forwarded

Dr. Biplab Biswas
(Supervisor)

Dr. Biplab Biswas
Assistant Professor
Department of Chemistry
Presidency University, Kolkata-700 073

Signature of the candidate

(Arindam Das)

Dr. Dhruba Prosad Chatterjee
(Co-Supervisor)

Chhanda Mukhopadhyay 18/9/24

Sujoy Baitalik 18/09/2024

18/09/2024

Adity Bose 18/9/24

18/9/24